Progress in the Next Linear Collider Design[1]

T.O. Raubenheimer[2]

Stanford Linear Accelerator Center, Stanford University, Stanford, California 94309 USA

Abstract. An electron/positron linear collider with a center-of-mass energy between 0.5 and 1 TeV would be an important complement to the physics program of the LHC. The Next Linear Collider (NLC) is being designed by a US collaboration (FNAL, LBNL, LLNL, and SLAC) which is working closely with the Japanese collaboration that is designing the Japanese Linear Collider (JLC). The NLC main linacs are based on normal conducting 11 GHz rf. This paper will discuss the technical difficulties encountered as well as the many changes that have been made to the NLC design over the last year. These changes include improvements to the X-band rf system as well as modifications to the injector and the beam delivery system. They are based on new conceptual solutions as well as results from the R&D programs which have exceeded initial specifications. The net effect has been to reduce the length of the collider from about 32 km to 25 km and to reduce the number of klystrons and modulators by a factor of two. Together these lead to significant cost savings.

I INTRODUCTION

The Next Linear Collider (NLC) [1,2] is a future electron/positron collider that is based on copper accelerator structures powered with 11.4 GHz X-band rf. It is designed to begin operation with a center-of-mass energy of 500 GeV or less, depending on the physics interest, and to be adiabatically upgraded to 1 TeV cms. A schematic of the NLC, which is not to scale, is shown in Fig. 1. The collider consists of electron and positron sources, two X-band main linacs, and a beam delivery system to focus the beams to the desired small spot sizes. The facility is roughly 26 km in length and supports two independent interaction regions (IRs).

The NLC proposal was started by SLAC and later joined by LBNL, LLNL, and FNAL. Work at Fermilab is just starting and will focus on the main linac beam line while the efforts at LBNL and LLNL are focused on the damping ring complex, the modulator systems and the gamma-gamma interaction region. In addition, there has been a close collaboration with KEK for several years concentrated on X-band rf development. The JLC linear collider [3] and the NLC have developed a set of

---

1) Work supported by the U.S. Department of Energy, Contact Number DE-AC03-76SF00515.
2) e-mail: tor@slac.stanford.edu

common parameters with very similar rf systems; a status report on the progress of this collaboration was published in 2000 [4].

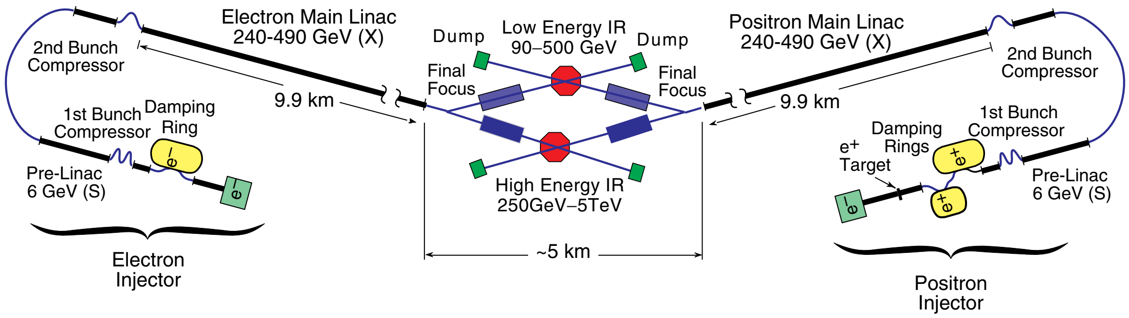

FIGURE 1. Schematic of the NLC (not to scale).

In May 1999 for a major DOE review, the NLC project presented both the technical design and a conservative cost estimate for the project. The reviewers concluded that the technical design was in good shape but questioned the viability of the project with the estimated total project cost. Over the last year, the NLC collaboration has concentrated on cost reduction and has been able to lower the original estimate by roughly 30%. In addition, the design has been further optimized to meet the physics requirements and there has been continued R&D on key technical components.

In the following, we will first describe recent developments in the NLC rf systems as well as the high power rf damage that has recently been observed in the accelerator structures. Next, we will discuss the modifications that have been made to the optical design including modifications to the collider layout that could allow the facility to collide beams with energies as high as 5 TeV once the appropriate rf systems are developed. Finally, we will discuss the NLC luminosity expectations and our future plans.

II X-BAND RF SYSTEM

The rf system for the NLC design operates at a frequency of 11.424 GHz to support the higher acceleration gradients needed for TeV-scale colliders. The rf system consists of four main components: the modulators which convert the line ac into pulsed dc power for the klystrons, the klystrons which convert the dc pulses into rf pulses at 11 GHz, the pulse compression system which temporally compresses the rf pulse while increasing the peak power, and the accelerator structures which transfer the rf power to the particle beam.

Currently, the NLC rf system is in its third design iteration. The evolution of the rf system has been driven by costing models that have been developed for the collider and by the results from the ongoing R&D programs. The first iteration of the rf system was based on conventional thyratron switched modulators, 50 MW Periodic Permanent Magnet (PPM) focused klystrons, the SLED-II pulse compression system and a Damped-Detuned (DDS) accelerator structure. This configuration was described in the NLC ZDR [1] and is the technology used in the NLC Test Accelerator (NLCTA). The NLCTA began operation in 1997 and verified the beam loading compensation scheme to be used in the NLC as well as the basic rf configuration [5].

The next iteration of the rf design was based on a 75 MW PPM X-band klystron, the Rounded DDS (RDDS) accelerator structure which has 12% higher shunt impedance and the Delay Line Distribution System (DLDS) pulse compression scheme which has significantly higher efficiency than the SLED-II system. This system still used the conventional PFN-type modulators and was presented at the 1999 NLC DOE review; it is described in Ref. [6].

The most recent iteration of the rf design is based on solid-state modulators with an rf pulse length of $3\,\mu$s instead of $1.5\,\mu$s from the klystrons. This longer pulse length reduces the required number of klystrons and modulators by a factor of two. In addition, the rf system uses an enhancement of the DLDS scheme where the rf power is propagated in two orthogonal modes to reduce the amount of waveguide required. In this current design, the rf system for each 250 GeV linac consists of 99 modules each of which contains a modulator, eight 75 MW X-band klystrons, an rf pulse compression unit, and 24 accelerator structures.

The present cost estimate for the rf system has decreased by roughly 50% from that in the 1996 cost model. In the following, we will discuss each of the components in more detail. We will also discuss some of the rf damage effects that have been observed in the X-band accelerator structures which may limit the gradient of the main linacs.

A Solid State Modulator

The NLC klystrons require roughly 250 Amps at 500 kV. The 1999 baseline cost model was based on a conventional PFN-type modulator which powered two klystrons at once. This was a conservative technology choice however the modulators had a relatively poor efficiency of roughly $65 \sim 70\%$ and they were clearly the most expensive component of the rf system.

Recent improvements in high power Isolated Gate Bipolar Transistor (IGBT) switches have made it possible to consider a solid state modulator design. These switches have relatively fast rise and fall times (<200ns) and can switch a few kA at a few kV [7]. The voltage contributions from a number of switches can be added together inductively in a manner similar to that in an induction linac. The NLC design uses a stack of 80 induction cores, each with two IGBT switches and a 3-turn transformer to generate over 2 kA at 500 kV. This modulator will drive 8 klystrons at once with an estimated cost that is roughly half the cost of the conventional modulator and with an overall efficiency greater than 75%.

In addition to the improved efficiency and reduced cost, the solid-state modulators have a number of other advantages. First, the reliability of the system has the potential to be much higher; failure of a single IGBT should be benign since the core saturates and becomes nearly transparent to the pulse. Additional cores and IGBTs will be included to offset such a loss. Second, the IGBTs will be independently timed to allow for pulse shaping and, for example, offset the natural droop of the pulse as the capacitors discharge.

At this time, a stack of 10 induction cores has been assembled and is being used to power a SLAC 5045 S-band klystron [8]. A full stack of 80 induction cores is being assembled and will be tested in the winter of 2001.

B 75 MW PPM X-band Klystrons

Conventional klystrons use a large solenoid magnet to focus the beam between the gun and the collector. Unfortunately, the magnet requires 20 kW of power which is comparable to the average rf output power, effectively decreasing the klystron efficiency. To avoid this a new generation of klystrons using periodic permanent magnet (PPM) focusing have been developed. In these PPM klystrons, the focusing is generated with rings of permanent magnet material which are interleaved with iron pole pieces to generate a periodic axial field.

In 1996, SLAC built a 50 MW PPM klystron which produced 2 μs long 50 MW pulses with a 55% efficiency. Next, a 75 MW PPM tube was built and was able to produce over 75 MW with a pulse length of 2.8 μs and an efficiency of roughly 55%, consistent with simulations [9]. At this output level, the pulse length was limited by the modulator output and the repetition rate was limited to 10 Hz due to inadequate cooling of the klystron. A second 75 MW PPM klystron is now being constructed to operate at the full 3 μs pulse length and 120 Hz repetition rate.

C Delay Line Distribution System

The klystrons most efficiently generate a lower power and longer pulse than that needed in the structures to accelerate the beam. To optimize the system, the rf pulse must be compressed temporally before being sent to the accelerator structures. The SLED-II system, in operation at the NLCTA, compresses the klystron pulse by a factor of 6 but the efficiency is only about 70% so the peak power is only increased by a factor of 4.

To improve on this efficiency, the DLDS system was proposed at KEK [10]. In this system, the power from eight klystrons is summed and divided into equal time intervals. It is then distributed up-beam to eight sets of accelerator structures that are spaced appropriately so that the beam-to-rf arrival time is the same in each case. The power is directed to each different group of structures by varying the relative rf phases of the eight klystrons. The intrinsic efficiency of this system is 100% although wall losses and fabrication errors will likely reduce that to 85 $\sim$ 90%.

To reduce the length of waveguide required, a multi-mode version of this system has been developed in which the power is distributed through a single circular waveguide, but in two or more different modes. In the current configuration, each waveguide transports two modes, reducing the length of waveguide by roughly a factor of two. Future studies will investigate both the possibility of transporting four modes in one waveguide and the utility of active rf switching techniques which might allow all the power to be transported in a single waveguide. Finally, to test the components at their design power levels, the NLCTA has been upgraded to produce 240 ns long pulses of 800 MW and testing will begin at the end of FY01.

D Accelerator Structures

The accelerator structures for NLC have been studied for many years, much of this in collaboration with KEK. A good summary of the structure development history is given in Ref. [11]. There are three requirements on the structure design: first it must transfer the rf energy to the beam efficiently, second, it must be optimized to reduce the short-range wakefields which depend on the average iris radius, and third, the long-range transverse wakefield must be suppressed to prevent multibunch beam breakup (BBU). The current design for the structures is a 1.8-m traveling wave structure consisting of 206 separate cells.

To optimize the rf efficiency, the structure cells are rounded, reducing the linac length by roughly 6% when compared to a simple disk-loaded waveguide like that in the SLAC linac. In addition, the long-range transverse wakefield is suppressed through a combination of detuning the dipole modes and weak damping. The damping is achieved through the addition of four single-moded waveguides (manifolds) that run parallel to the structure and couple to the cells through slots. The signals from this manifold also can be used to determine the beam position with respect to the accelerator structure to micron-level accuracy. Finally, to reduce the short-range wakefields, the average iris radius is $a/\lambda \sim 0.18$, leading to a relatively large group velocity ranging from 12% in the front of the structure to 2% at the exit.

Four of these damped-detuned accelerator structures (DDS) have been built with the most recent structure using rounded cells. Measurements of the rf properties of the structures [12,13] have confirmed: (1) the cell fabrication techniques which can achieve sub-MHz accuracy, (2) the wakefield models and wakefield suppression techniques, (3) the rf BPMs which are necessary to align the structures to the beam and prevent emittance dilution, and (4) the rf design codes which have sub-MHz accuracy [14].

E High Power Damage

Although most of the structure R&D results have been very positive, we have also uncovered a major problem in the structure design. The NLC design calls for a gradient of 70 MV/m to attain a center-of-mass energy of 1 TeV with a reasonable length linac. In the past, we have tested a number of short X-band structures at gradients of over 100 MV/m but it is only recently that we have has sufficient rf power to test the full 1.8 m structures at their design gradient. During these recent tests, damage has been observed after 500 hours of operation. The onset of damage appears to occur at a gradient of $40 \sim 50\,\mathrm{MV/m}$ [15]. At this time, it is not known if this damage is the result of our structure fabrication techniques, our rf processing methods, or something more fundamental to the present structure design.

The two primary differences between the present structures and those tested earlier at much higher gradients is the structure length and the group velocity of the rf power in the structure. A simple theoretical model has been developed which may explain the correlation with group velocity [16]. More recently, a workshop was held at SLAC [17] to discuss the breakdown phenomena and the world-wide R&D on high gradient acceleration.

To study the gradient limitation, SLAC and KEK are constructing 12 structures with different group velocities and lengths. In addition, one of the 1.8-m structures has been cut in two and the last $\frac{1}{3}$ of the structure, where the maximum group velocity is 5%, is being tested. This shortened structure has reached a gradient of 70 MV/m roughly 10 times faster than the full length structures and, after about 1000 hours of operation, no evidence of rf damage has been observed—a very encouraging initial result! In addition, we are studying different cleaning techniques during fabrication and different processing methods as well as the different structure designs. Finally, working on the assumption that the correlation of gradient with group velocity is correct, we are in the process of designing a replacement structure for the NLC which we could construct quickly if the testing confirms the initial results. The replacement structure has a lower group velocity which is attained with a phase advance of 150° per cell instead of the standard 120° [18] to keep the average iris radius large.

III OPTICAL DESIGN CHANGES

Over the last year, a number of changes have also been made to the optical design to reduce the collider cost and/or improve the collider performance. In this section, we will discuss the changes to the beam delivery system (BDS) which includes a new design for the beam collimation system, a new final focus design, and a new interaction region layout. All of these systems have been completely redesigned over the last year, resulting in a BDS design that is more robust and is half the length of that presented in 1999. The resulting site footprint is roughly 26 km in length rather than 32 km. Other changes which will not be discussed include extensive use of permanent magnets [19], modifications to the bunch compressor system [20], small changes to the beam parameters, possibly placing much of the control electronics directly into the linac tunnels, and modified civil construction techniques to reduce costs.

A Beam Collimation System

The beam collimation system has two purposes: it must collimate the beam tails to prevent backgrounds at the IP, including those generated by the collimation system itself, and it must protect the downstream components against errant beams. In the previous design, the beam collimation section was designed to survive any mis-steered or off-energy incoming beam. This is a difficult constraint because the beam density is normally so high that the beam will damage any material intercepted [21]. The resulting collimation design had to be roughly 2.5 km to collimate 500 GeV beams and the system energy bandwidth was only 1% with very tight optical tolerances—so tight that very small misalignments within the system could cause the beams to damage the beam line components.

In a pulsed linac, the beam energy can change from pulse-to-pulse however large changes to the beam trajectory which are not due to energy errors are much less frequent. We have taken advantage of this fact and redesigned the collimation system to passively survive any off-energy beam but to allow on-energy beams with large betatron errors to damage the collimators. The betatron collimators will be 'consumable' collimators which can be rotated to a new position after being damaged [22]; based on SLC experience, we expect the frequency of the errant betatron errors to be much less than 1000 times per year. The net effect of this change in the design specification is that we now have a design that is roughly half as long with much looser tolerances and a larger bandwidth [23,24].

The 1999 collimation system was also designed to remove tails consisting of 1% of the beam. This number was based on some of the poorer SLC operation despite the fact that simulations predict tails that are less than 0.0001% of the beam. Much of the beam tail in the SLC is thought to originate in the damping rings and the bunch compressor. In the current design, we have included a low energy collimation system to remove these tails at 8 GeV that is much easier to design than the high energy system. This allows us to reduce the maximum number of particles the high energy system must remove from 1% to 0.1% of the beam which is still 1000 times more than that expected. Although it may seem excessive to over-design the collimation system by such a large factor, adequate beam collimation is absolutely essential for the particle detector to log data and retrofitting a system for additional collimation as was done in the SLC is a difficult and expensive task.

B Final Focus

In addition to the beam collimation system, we have completely redesigned the final focus system (FFS). The previous FFS was based on the lattice of the Final Focus Test Beam (FFTB) at SLAC which was constructed from separate modules for the chromatic correction and made full use of symmetry. Although this makes the design of the FFS simpler, it has the disadvantage of making the FFS quite long—1.8 km for 750 GeV beams.

A new design has been adopted where the chromatic correction of the strong final magnets is performed locally at these magnets [25]. This results in a compact design with many fewer elements which has better performance than the previous version. In particular, the new FFS has a larger energy bandpass with comparable alignment tolerances and a more linear transport which should make it less sensitive to beam tails. Because of the better performance, we have actually increased $L^\star$, the free space from the final magnet to the IP, from 2-m to 4.3-m; this will simplify the design of the interaction region and the interface with the high-energy physics detector.

Finally, the scaling of the length with beam energy in this new design is much weaker than in the earlier design. The present FFS is only 700 m in length but can focus 2.5 TeV beams while an equivalent conventional design would have to be roughly 10 km in length. This change makes it much more reasonable to consider a multi-TeV collider using an advanced high-gradient rf system such as the CLIC design [26]; otherwise the FFS is longer than the linacs.

C Interaction Region Layout

A normal conducting linear collider has relatively tightly spaced bunches and must collide the beams with a crossing angle; the crossing angle reduces the parasitic collisions between bunches that are not at the IP and greatly facilitates the extraction of the disrupted beam after collision. The crossing angle for e^+/e^- or e^-/e^- collisions in the NLC and CLIC designs is 20 mrad while a larger angle of roughly 30 mrad would be desired for the γ/γ IR because of the larger disruption of the beam. In our previous design, we had two collinear linear accelerators aimed directly at each other and the beams were bent through an angle of 10 mrad to develop the 20 mrad crossing angle. Unfortunately, this bending limits the energy reach of the BDS because the synchrotron radiation dilutes the beam emittance.

We have taken advantage of the higher energy reach of the new FFS, discussed in the previous section, by eliminating the bending between the main linacs and one of the two IRs, referred to as the High Energy IR (HEIR). This prevents the synchrotron radiation emittance dilution in a very high energy beam. Thus, the two linacs still point at each other but are now orientated with a 20 mrad crossing angle as illustrated in Fig. 1. With this layout, the NLC could be upgraded to a multi-TeV facility in a cost effective manner, reusing much of the infrastructure and beam line components, once a high gradient rf system, such as that being pursued at CERN for the CLIC design, is developed.

Now, the second IR will be separated transversely from the HEIR by arcs that will generate a 30 mrad crossing angle and will provide sufficient transverse separation to avoid interference with the HEIR. This second IR is referred to as the Low Energy IR (LEIR) although it should be noted that for most of the NLC operation the distinction between the HEIR and LEIR is not necessarily important. The LEIR will have very comparable luminosity performance up to a maximum center-of-mass collision energy which is between 500 GeV and 1 TeV—the exact value will be determined depending on the physics interest. However, the operating range of a final focus beam line is limited to roughly a factor of five in beam energy without needing modification of the components. Thus, we are presently assuming that the FFS of the LEIR will be optimized to operate between roughly 90 and 500 GeV while the FFS of the HEIR would be optimized for operation between 250 GeV and 1 TeV. This will provide overlapping coverage over the full energy range between the Z-pole and 1 TeV collisions.

IV ENERGY EVOLUTION

The NLC is optimized to operate with a collision energy of 1 TeV in the center-of-mass (cms). To accelerate the beams to 500 GeV (for 1 TeV collisions) the linacs must be roughly 10 km in length. However, to reduce the initial facility cost and to more quickly address the physics of immediate interest, the NLC would start colliding beams with a cms energy of 500 GeV. In this initial configuration, the full beam line tunnels would be constructed but rf components would only be installed in half of the tunnels. It would then be straightforward to upgrade the facility to the full energy of 1 TeV by installing additional rf components.

Thus, we envision two stages for the facility: 500 GeV collisions initially and 1 TeV collisions later. Of course, as discussed in the previous section, the facility is being designed with the capability of supporting multi-TeV collisions in the future after the appropriate rf technology is developed. In addition, it may be possible to reach higher collision energies with the same X-band technology by either extending the linac length or by increasing the accelerating gradient. To this end, most of both the BDS and the injector system components have been specified to support the 750 GeV beams however neither of these upgrade options are assured.

V LUMINOSITY

The NLC was initially designed to provide a luminosity greater than $5 \times 10^{33}\,\mathrm{cm}^{-2}\mathrm{s}^{-1}$ at a center-of-mass energy of 500 GeV and a luminosity in excess of $10 \times 10^{33}\,\mathrm{cm}^{-2}\mathrm{s}^{-1}$ at 1 TeV cms [2]. To ensure this luminosity, the design included a large operating space with numerous margins and overheads. For example, the injector system has been specified to produce roughly 50% more charge than required. Similarly, the beam emittance dilution budgets, which were in excess of 300%, were based on the component tolerance specifications without consideration of the emittance tuning techniques pioneered at the Stanford Linear Collider (SLC) [27]; at the SLC, the emittance tuning techniques reduced the emittance dilutions by an order-of-magnitude.

At Snowmass '96, we estimated the luminosity that could be expected if all of the collider subsystems performed as specified. This luminosity is roughly a factor of four higher than the nominal luminosity and is similar to the TESLA luminosity values which are based on similar assumptions. One way to state the expected luminosity of the collider is to discuss the *intrinsic*, the *design*, and the *initial* luminosities which are defined as follows:

- **intrinsic**—the luminosity limited only by physical effects such as synchrotron radiation, beam space charge, and the beam-beam interaction
- **design**—the luminosity assuming that all components perform as designed including the beam tuning techniques
- **initial**—the initial luminosity of the collider which is expected to be attained at turn-on

These values for the 500 GeV cms collider are listed in Table 1. It is important to note that the intrinsic luminosity of the collider is roughly twice the design value and the design value is roughly four times the initial specification of 5×10^{33}.

A set of design parameters for the NLC at different energies are listed in Table 2. The first two columns list the luminosity and IP parameters for Stage 1 (500 GeV cms) and Stage 2 (1 TeV cms) operation while the last three list luminosity at lower collision energies. Note that the energy in Stage 1 and Stage 2 is lower than the nominal 500 GeV or 1 TeV. This arises because of the beam loading—the same

TABLE 1. Comparison of intrinsic, design, and initial vertical emittance $\gamma\epsilon_x$ / $\gamma\epsilon_y$ and luminosities at 500 GeV cms

	Intrinsic	Design	Initial
Damping Ring [10^{-8} m-rad]	300 / 1	300 / 2	300 / 3
Main Linacs [10^{-8} m-rad]	315 / 1	330 / 3.5	400 / 8
Beam Delivery [10^{-8} m-rad]	330 / 1	360 / 3.5	450 / 8
Luminosity [$\mathrm{cm}^{-2}\mathrm{s}^{-1}$]	45×10^{33}	22×10^{33}	6×10^{33}

TABLE 2. A set of IP design parameters

	High Energy IP		Low Energy IP		
CMS Energy [GeV]	888[a]	446[b]	350	250	90
Luminosity [$10^{33}\,\mathrm{cm}^{-2}\mathrm{s}^{-1}$]	34	20	13	9	3.5
Repetition rate [Hz]	120	120	120	120	120
Bunch Charge [10^{10}]	0.75	0.75	0.75	0.75	0.75
Bunches per pulse	190	190	190	190	190
Bunch separation [ns]	1.4	1.4	1.4	1.4	1.4
IP $\gamma\epsilon_x/\gamma\epsilon_y$ [10^{-8} m-rad]	360 / 3.5	360 / 3.5	360 / 3.5	360 / 3.5	360 / 3.5
IP σ_x/σ_y [nm]	200 / 2.2	260 / 2.8	320 / 3.2	380 / 3.8	630 / 6.2
Beamstrahlung [%]	8.8	4.6	2.0	1.1	0.18

[a] Stage 2 operation—energy is lower than 1 TeV due to beam loading
[b] Stage 1 operation—energy is lower than 500 GeV due to beam loading

effect that allowed LEP to reach it highest energies as the beam current decayed. In the Stage 2 NLC, the luminosity varies from 34×10^{33} at 890 GeV to 22×10^{33} at 1 TeV; the percentage change in the Stage 1 is similar. It will be an operational decision as to how best to balance this energy/luminosity trade.

Usually, the largest concern regarding the luminosity performance in the NLC relates to the emittance preservation because the wakefields in the high frequency linacs are much stronger than in lower frequency designs. However, it should be noted that the beam parameters of the NLC have been chosen so that the *effect* of the wakefields on the beam dynamics is roughly 25% of that in the SLC linac. This was done by making the bunch charge and bunch length smaller and the transverse focusing stronger. This reduction in the effect of the wakefields will make the beam much more stable and much easier to control than it was in the SLC.

Regardless, to preserve the beam emittance, the tolerances in the NLC are very tight. Typical alignment tolerances on the accelerator structures are $10\,\mu$m while those on the quadrupoles are $1\,\mu$m. These tolerances *must* be attained using beam-based alignment techniques and constant feedback. Such an approach is straightforward *provided* the diagnostics and the controls can be developed with sufficient resolution—much more difficult control problems are performed in jet aircraft all the time! The importance of the diagnostics was one of the key lessons from the SLC operation [27].

Many of the required diagnostics and controls were developed for the Final Focus Test Beam at SLAC and have been repeatedly demonstrated during operation

[28–30]. More recently, many of the component prototypes for NLC have returned results that are much better than the initial specifications. For example, if the rf structure BPMs perform as measured in the DDS3 and RDDS1 structures [12,13], the emittance dilution due to wakefields would decrease from the allocated 50% to less than 10%. Furthermore, these tolerances do not assume the use of the emittance correction techniques that were developed during the SLC operation. In the SLC, the components had to be aligned mechanically and the resulting emittance dilutions were quite large. However, emittance correction techniques which modified the beam trajectory were used to reduce the emittance dilution by an order-of-magnitude. These techniques will be used on top of the direct beam-based alignment approaches.

It is always difficult to know exactly how quickly a new facility can be commissioned. However, the most important point for the NLC commissioning is that the NLC is a *2nd generation* linear collider and all of the techniques needed have been developed in the SLC or the other test facilities. Because it is a 2nd generation facility and because of the built-in margins, we are very confident that the collider will turn-on rapidly, exceeding the initial goals, and would reach the design performance after one of two years of operation. To this end, we can specify an integrated luminosity over a three or four year run of 500 fb^{-1} for Stage 1 and 1000 fb^{-1} for Stage 2.

VI SUMMARY

Over the last year, the NLC collaboration has been focused on new technology developments and design changes to reduce the facility cost. We are making extensive changes to our baseline rf system and to the beam line optics, reducing the collider footprint from 32 km to 26 km while maintaining the energy reach of the facility. We have also uncovered a high gradient limitation in our accelerator structure design and are vigorously investigating solutions—although earlier structure designs have operated at gradients well over 100 MV/m, the present structures are limited to gradients between 40 and 50 MV/m. Finally, we have modified the collider layout so that it does not preclude upgrading the facility to a multi-TeV collider once an appropriate rf system has been developed.

REFERENCES

1. NLC ZDR Design Group, SLAC Report-474 (1996).
2. http://www-project.slac.stanford.edu/lc/NLC-tech.html.
3. N. Toge, "JLC Progress," *Invited paper at the 20th Int. Linear Acc. Conf.*, Monterey, CA (2000).
4. International Study Group, N. Toge, ed., "International study group progress report on linear collider development," KEK 2000–7, SLAC–R–559 (2000).
5. R.D. Ruth *et al.*, "Results from the SLAC NLC test accelerator," *Proc. of the 1997 IEEE Part. Acc. Conf.*, Vancouver, Canada (1997).
6. C. Adolphsen, "Research and Development for an X-Band Linear Collider," *Invited paper at the 19th Int. Linear Acc. Conf.*, Chicago, IL (1998).
7. E. Cook, "Review of Solid-State Modulators," *Invited paper at the 20th Int. Linear Acc. Conf.*, Monterey, CA (2000).

8. R.L. Cassel, *et al.,* “Solid-State Induction Modulator Replacement for the Conventional SLAC 5045-Klystron Modulators,” *Proc. of the 20th Int. Linear Acc. Conf.*, Monterey, CA (2000).
9. E. Jongewaard, *et al.,* “Next Linear Collider Klystron Development Program,” *Proc. of the 20th Int. Linear Acc. Conf.*, Monterey, CA (2000).
10. S. Tantawi, “New Development in RF Pulse Compression,” *Invited paper at the 20th Int. Linear Acc. Conf.*, Monterey, CA (2000).
11. J. Wang, *et al.,* “Accelerator Structure R&D for Linear Colliders,” *Proc. of the 1999 IEEE Part. Acc. Conf.*, New York, NY (1999) p. 3423.
12. C. Adolphsen, *et al.,* ”Wakefield and Beam Centering Measurements of a Damped and Detuned X-Band Accelerator Structure,” *Proc. of the 1999 IEEE Part. Acc. Conf.*, New York, NY (1999) p. 3477.
13. J. Wang, *et al.*, “Design, Fabrication and Measurement of the First Rounded Damped Detuned Accelerator Structure (RDDS1),” *Proc. of the 20th Int. Linear Acc. Conf.*, Monterey, CA (2000).
14. N. Folwell, *et al.,* “SLAC Parallel Electro-magnetic Code Development and Applications,” *Proc. of the 20th Int. Linear Acc. Conf.*, Monterey, CA (2000).
15. C. Adolphsen, *et al.,* “RF Processing of X-band Accelerator Structures at the NLCTA,” *Proc. of the 20th Int. Linear Acc. Conf.*, Monterey, CA (2000).
16. C. Adolphsen, C. Nantista, “Simulations of RF Breakdown in X-band Accelerator Structures and its Implications for the Design of High-Gradient Structures,” *Proc. of the 20th Int. Linear Acc. Conf.*, Monterey, CA (2000).
17. *Structure Breakdown Workshop*, SLAC, August 28–30, 2000, http://www-project.slac.stanford.edu/lc/wkshp/RFBreakdwn/struct_breakdown_wrkshp.htm
18. Z. Li, N. Folwell, T.O. Raubenheimer, “Numerical Studies on Locally Damped Structures,” *Proc. of the 20th Int. Linear Acc. Conf.*, Monterey, CA (2000).
19. H.D. Glass, ”Permanent Magnets for Beam-lines and the Recycler Ring at Fermilab,” *Invited talk at 17th Int. Conf. on High-Energy Acc.,* Dubna, Russia (1998).
20. P. Emma, “Cost and Performance Optimization of the NLC Bunch Compressor Systems,” SLAC LCC-0021 (1999).
21. M.C. Ross, *et al.,* “Single Pulse Damage in Copper,” *Proc. of the 20th Int. Linear Acc. Conf.*, Monterey, CA (2000).
22. J. Frisch, E. Doyle, K. Skarpas, “Advanced Collimator Systems for the NLC,” *Proc. of the 20th Int. Linear Acc. Conf.*, Monterey, CA (2000).
23. P. Tenenbaum, *et al.,* “Studies of Beam Optics and Scattering in the Next Linear Collider Post-Linac Collimation System,” *Proc. of the 20th Int. Linear Acc. Conf.*, Monterey, CA (2000).
24. P. Tenenbaum, *et al.,* “Direct Measurement of Geometric Wakefields from Tapered Rectangular Collimators,” *Proc. of the 20th Int. Linear Acc. Conf.*, Monterey, CA (2000).
25. P. Raimondi, “New Developments in Linear Collider Final Focus Systems,” *Invited paper at the 20th Int. Linear Acc. Conf.*, Monterey, CA (2000).
26. J.P. Delahaye, “CLIC, a Two-Beam e^+e^- Linear Collider in the TeV Range,” *Invited paper at the 20th Int. Linear Acc. Conf.*, Monterey, CA (2000).
27. N. Phinney, “SLC Final Performance and Lessons,” *Invited paper at the 20th Int. Linear Acc. Conf.*, Monterey, CA (2000).
28. S. Smith, P. Tenenbaum and S. H. Williams, “Performance of the beam position monitor system of the final focus test beam,” Nucl. Instr. Meth. **A431**, 9 (1999).
29. T. Slaton, G. Mazaheri and T. Shintake, “Development of nanometer resolution C-band radio frequency beam position monitors in the final focus test beam,” SLAC-PUB-7921 *Talk given at 19th International Linear Accelerator Conference (Linac 98), Chicago, IL, 23-28 Aug 1998.*
30. G. Bowden, P. Holik, S. R. Wagner, G. Heimlinger and R. Settles, “Precision magnet movers for the final focus test beam,” Nucl. Instr. Meth. **A368**, 579 (1996).